Fatigue Fracture Planes and the Critical Plane Orientations in Multiaxial Fatigue Failure Criteria

A. Karolczuk and E. Macha

Opole University of Technology, Faculty of Mechanical Engineering, ul. Mikolajczyka 5, 45-271 Opole, Poland, karol@po.opole.pl, emac@po.opole.pl

ABSTRACT. *This paper deals with the problem of the critical plane determination for multiaxial fatigue failure criteria. Experimental results from multiaxial proportional, non-proportional cyclic loading and variable-amplitude bending and torsion were used to determine the macroscopic fracture plane orientations and the fatigue lives. Some known multiaxial critical plane criteria were verified based on the fracture plane orientations and experimental fatigue lives. It was concluded that frequently the critical and fracture plane orientations do not coincide. However, the morphology of fracture planes is a key for an appropriate choice of the fatigue failure criterion for the fatigue life estimation.*

INTRODUCTION

Various multiaxial fatigue failure criteria based on the critical plane approach have been proposed [1-8]. This approach is based upon the experimental observation that fatigue cracks initiate and grow on certain material planes. Therefore, it is assumed that only stress or/and strain components acting on the critical plane are responsible for the material fatigue failure. The critical plane criteria define different functions that combine the shear and normal stress or/and strain components on a plane into one equivalent parameter called damage parameter. It is commonly accepted that depends on loading level, temperature, material type, state of stress, materials generally form one of the two types of cracks - shear cracks or tensile cracks. Hence, the equivalent damage parameter is usually compared to the uniaxial shear or tensile damage parameter obtained by the experimental tests under torsion or push-pull loading. However, it is also accepted that either under multiaxial and uniaxial fatigue tests the cracks may initiate and propagate on different planes – contradictory to the one critical plane orientation. The following conclusion appears: the critical plane and the fracture plane notions must be separated. The critical plane is simply a plane that is used in the fatigue life assessment. The fracture plane at the microscale/macroscale is a plane where material cohesion is lost. Depending on loading levels, state of stress etc. the critical plane and fracture plane orientations may or not coincide.

We postulate that the critical plane approach may be successfully used in the fatigue life estimation under different test conditions but the proposed damage parameter should be equivalent to the uniaxial one not only in term of the total fatigue life but also

in term of the macroscopic fracture plane behaviour. For example, if under uniaxial torsion loading for a given fatigue life, some macroscopic cracks coincide with the maximum shear stress plane and other with the maximum normal stress plane than the fatigue criterion based on the torsion S-N curve should be used in the fatigue life estimation if the same fracture behaviour is revealed under multiaxial loading.

A BRIEF REVIEW OF SOME MULTIAXIAL FATIGUE FAILURE CRITERIA BASED ON THE CRITICAL PLANE APPROACH

According to the critical plane approach, the fatigue failure of the material is due to the stress or/and strain hostories acting on the critical plane. Different functions of these components on the critical plane (with normal $\vec{n}$ and shear $\vec{s}$ unit vectors) were proposed. Fatigue failure occurs if the following general expression is fulfilled:

$$F[\sigma_n(t), \tau_{ns}(t), \varepsilon_n(t), \varepsilon_{ns}(t), K] > Q\,, \tag{1}$$

where: σ_n, τ_{ns} are the normal and shear stress components on the critical plane; ε_n, ε_{ns} are the normal and shear strain components on the critical plane; K is the material coefficient set; Q is the fatigue limit. For a limit state of stress, the following general form of fatigue failure can be presented

$$F[\sigma_n(t), \tau_{ns}(t), \varepsilon_n(t), \varepsilon_{ns}(t), K] = q\,, \tag{2}$$

where q is the material parameter for a given number of cycles to failure.

Some multiaxial critical plane criteria applicable to the cyclic loading are presented and adapted to variable-amplitude loading.

The Findley Criterion

Findley [2] proposed a linear combination of the maximum normal stress $\sigma_{n,\max}$ and the shear stress amplitude $\tau_{ns,a}$ on the critical plane for a given number of cycles to failure N_f

$$\tau_{ns,a} + k\sigma_{n,\max} = f\,, \tag{3}$$

where f and k are the material coefficients. The critical plane orientation coincides with the plane orientation where the maximum value of this linear combination occurs. It depends on the material coefficient k. Findley noticed that k value was small for ductile materials and the position of the critical plane for these materials approached to the direction of maximum shear stress. A high k value is characteristic for brittle materials like cast iron, and the critical plane position is then compatible with the position of maximum principal stress direction σ_1. Findley did not define a mathematical formula for the material coefficient f. Some researchers [3-4] assume that it can be determined from the shear-mode cracking

$$\tau_{ns,a} + k\sigma_{n,\max} = \tau_{af}\left(\frac{N_\tau}{N_f}\right)^{1/m_\tau}, \tag{4}$$

where τ_{af}, m_τ are the fatigue limit and the exponent of the S-N curve for fully reversed (R=-1) torsion loading, respectively; N_f is the considered number of cycles to failure; N_τ is the number of cycles corresponding to the fatigue limit τ_{af} for fully reversed torsion loading.

The Findley criterion and others are based on the cyclic properties of fatigue loading for which the amplitude of the shear stress τ_{ns}(t) can be found. The problem appears under random loading. Some authors [5, 6] proposed to extract the amplitudes by the rainflow method taking the normal stress component σ_n(t) or the shear stress component τ_{ns}(t) as the cyclic counting variable and then the maximum or the amplitude of the remained loading component is calculated for each extracted cycle. However, such approach is complicated and time consuming since for every extracted cycle the two loading parameters (shear and normal) must be found. Nevertheless, it is possible to adapt Findley and other criteria to random loading. Our aim it to define the equivalent loading history based on the particular failure criterion. For the Findley criterion, the equivalent stress course is as follows

$$\tau_{eq}(t) = \tau_{ns}(t) + k\sigma_n(t). \tag{5}$$

The equivalent shear stress history τ_{eq}(t) at observation time T is then used as the cyclic counting variable. In this case, the range of amplitudes can be divided into the finite numbers of stress levels. For each *i-th* stress level $\tau_{eq,a}^{(i)}$, damage degree is computed by the general equation as follows

$$D^{(i)} = \begin{cases} \dfrac{n^{(i)}}{N_f^{(i)}} & for \quad F_{eq,a}^{(i)} \geq aF_{af} \\ 0 & for \quad F_{eq,a}^{(i)} < aF_{af} \end{cases}, \tag{6}$$

where F is the generalised fatigue damage parameter (for the Findley criterion: $F=\tau$), $n^{(i)}$ is the number of cycles assigned into the *i-th* stress level, a is a coefficient allowing to include amplitudes below F_{af} in the damage accumulation, $N_f^{(i)}$ is a computed number of cycles to failure for the *i-th* stress level (e.g. by Eq. (4)). It is assumed that $a = 0.5$ is sufficient, for lower value, the damage degree is too small to be taken into account. The proposed equivalent history must keep the frequency and the mean value of shear and normal loading components on the critical plane. It should be noted that under the proportional cyclic loading Eqs (4) and (5) result in the same damage degree. The critical plane orientation is determined by the maximum accumulated damage degree D

$$(\vec{n}, \vec{s}) : \max\{D\}. \tag{7}$$

The Matake Criterion

Matake [7] introduced a linear combination of the shear and normal stresses on the critical plane, similar to the Findley proposal

$$\tau_{ns,a} + k\sigma_{n,a} = \tau_{af}\left(\frac{N_\tau}{N_f}\right)^{1/m_\tau}, \tag{8}$$

where $\sigma_{n,a}$ is the normal stress amplitude on the critical plane. However, the critical plane orientation coincides with the maximum shear stress amplitude. For such orientation of the critical plane, it is possible to determine the material coefficient k. For uniaxial torsion loading, the plane of the maximum shear stress amplitude does not experience the normal stress. Therefore, the material coefficient k is determined from uniaxial push-pull tests. For fatigue limit, $\tau_{ns,a} = 0.5\sigma_{af}$, $\sigma_{n,a} = 0.5\sigma_{af}$; where σ_{af} is the fatigue limit under push-pull tests (R=-1). Eq. (8) takes the following form

$$\frac{1}{2}\sigma_{af} + k\frac{1}{2}\sigma_{af} = \tau_{af}. \tag{9}$$

From Eq. (9), the k coefficient is as follows

$$k = 2\frac{\tau_{af}}{\sigma_{af}} - 1. \tag{10}$$

Under random loading, the equivalent shear stress history has the same mathematical form as Eq. (5). However, for the Matake criterion the maximum shear stress range determines the critical plane orientation.

$$(\vec{n},\vec{s}) : \Delta\tau_{ns} = \max_{0<t<T}\{\tau_{ns}(t)\} - \min_{0<t<T}\{\tau_{ns}(t)\}, \tag{11}$$

where T is the time of observation. Damage degree $D^{(i)}$ is computed on the critical plane for each *i-th* stress level according to the general Eq. (6), where $F=\tau$.

The Maximum Normal Stress Criterion on the Critical Plane (max{σ_n})

This failure criterion comes from the static hypothesis of material strength. According to this criterion, the maximum normal stress range is responsible for the fatigue of materials. For the cyclic loading it leads to the following equation

$$\sigma_{n,a} = \sigma_{af}\left(\frac{N_\sigma}{N_f}\right)^{1/m_\sigma}, \tag{12}$$

where m_σ is the exponent of the S-N curve for fully reversed (R=-1) push-pull loading; N_σ is the number of cycles corresponding to the fatigue limit σ_{af}.

For random loading the equivalent stress history is as follows

$$\sigma_{eq}(t) = \sigma_n(t). \tag{13}$$

Damage degree $D^{(i)}$ is computed on the critical plane for each *i-th* stress level according to the general Eq. (6), where $F=\sigma$.

The Fatemi-Socie Criterion (FS)

Fatemi and Socie [8] observed the fatigue fractures and came into conclusion, that the normal stress σ_n on the maximum shear strain range plane accelerates the fatigue damage process through the crack opening. They proposed the following combination of the shear strain amplitude $\gamma_{ns,a}$ and the maximum normal stress $\sigma_{n,max}$

$$\gamma_{ns,a}\left(1+w\frac{\sigma_{n,\max}}{\sigma_y}\right) = (1+\nu)\frac{\sigma_f'}{E}(2N_f)^b + \frac{w}{2}(1+\nu)\frac{\sigma_f'^2}{E\sigma_y}(2N_f)^{2b} + 1.5\varepsilon_f'(2N_f)^c + \frac{w}{2}1.5\frac{\varepsilon_f'\sigma_f'}{\sigma_y}(2N_f)^{b+c}, \tag{14}$$

where ν is the Poisson's ratio, E is the Young's modulus, σ_y is the quasi-static yield stress, ε_f', c are the normal fatigue ductility coefficient and exponent, respectively, w is the material coefficient. The critical plane is the plane of the maximum shear strain amplitude $\gamma_{ns,a}$. The complicated right side of Eq. (14) comes from the decomposition of the total shear strain amplitude into elastic and plastic parts, which are then compared to the push-pull fatigue characteristics on the critical plane. Such methodology results in appearance of material coefficient w on both sides of Eq. (14).

For random loading, the following equivalent shear strain history is applied

$$\gamma_{eq}(t) = \gamma_{ns}(t)\left(1+w\frac{\sigma_{n,\max}}{\sigma_y}\right). \tag{15}$$

In Eq. (15), unlike in the previous criteria, the maximum normal stress $\sigma_{n,\max}$ on the critical plane is applied instead of the normal stress course $\sigma_n(t)$ to avoid nonlinearity in function for the equivalent shear strain history. The nonlinear function would not keep the mean value of strain and the frequency could be changed.

The critical plane orientation under random loading is the plane with the maximum shear strain range

$$(\vec{n},\vec{s}): \Delta\gamma_{ns} = \max_{0<t<T}\{\gamma_{ns}(t)\} - \min_{0<t<T}\{\gamma_{ns}(t)\}. \tag{16}$$

Damage degree $D^{(i)}$ is computed on the critical plane for each *i-th* stress level according to the general Eq. (6), where $F=\gamma$ with the assumption $\gamma_{af} = \tau_{af}/G$ (G is the Kirchhoff's modulus).

Damage Degree Accumulation and Fatigue Life Calculation

For the variable-amplitude loading, two linear damage accumulation hypotheses were applied: well known Palmgren-Miner hypothesis [9] and Sorensen-Kogayev hypothesis [10]. Both hypotheses may be written as follows

$$D = \frac{1}{p}\sum_{i=1}^{j} D^{(i)}, \tag{17}$$

where $D^{(i)}$ is the damage degree computed according to the general Eq. (6), p is the hypothesis coefficient, j is the total number of loading levels (we assume $j = 64$). For Palmgren-Miner hypothesis $p = 1$. For Serensen-Kogayev p is calculated according to the following equations:

$$p = \frac{\sum_{i=1}^{j} F_{eq,a}^{(i)} f^{(i)} - aF_{af}}{F_{eq,a}^{\max} - aF_{af}}, \quad f^{(i)} = \frac{n^{(i)}}{\sum_{i=1}^{j} n^{(i)}}, \tag{18}$$

where $f^{(i)}$ is the frequency of the *i-th* loading level, $F_{eq,a}^{\max}$ is the maximum amplitude of the generalised fatigue damage parameter ($F = \tau$, σ, or γ).

Accumulated damage degree D at observation time T is used to estimate the fatigue life according to the following expression

$$T_{cal} = \frac{T}{D(T)}, \tag{19}$$

In the case of the cyclic loading, the number of cycles to failure N_{exp} is computed directly from Eqs (4), (8), (12), (14) and then recalculated to

$$T_{cal} = \frac{N_{\exp}}{f}, \tag{20}$$

where f is the frequency of the cyclic loading.

FATIGUE TESTS

Detailed information about the experimental setup can be found in [11, 12]. Fatigue tests were performed on the round full cross-section specimen made of 18G2A steel in the high cycle fatigue regime (HCF) under constant- and variable-amplitude combined bending and torsion moment histories measurement (bending: $M_b(t)$, torsion: $M_t(t)$). The mechanical properties of the 18G2A steel are shown in Tab. 1.

Table 1. Mechanical properties of the 18G2A steel

Property	Value
Quasi-static yield stress, σ_y, Mpa	357
Ultimate strength, σ_u, Mpa	535
Young's modulus, E, Gpa	210
Poisson's ratio, ν	0.30
Fatigue limit for fully reversed torsion loading, τ_{af}, MPa (*)	142.5
Exponent of the S-N curve for fully reversed torsion loading, m_τ (*)	12.3
Number of cycles corresponding to the fatigue limit τ_{af} for fully reversed torsion loading, N_τ, cycles	$1.98 \cdot 10^6$
Fatigue limit for fully reversed push-pull loading, σ_{af}, Mpa	204
Exponent of the S-N curve for fully reversed push-pull loading, m_σ,	8.2
Number of cycles corresponding to the fatigue limit τ_{af} for fully reversed push-pull loading, N_σ, cycles	$1.24 \cdot 10^6$
Fatigue ductility coefficient for fully reversed push-pull loading, ε_f',	0.693
Fatigue ductility exponent for fully reversed push-pull loading, c,	-0.410
Fatigue strength coefficient for fully reversed push-pull loading, σ_f', MPa	782
Fatigue strength exponent for fully reversed push-pull loading, b,	-0.118
Cyclic hardening coefficient, K', Mpa	869
Cyclic hardening exponent, n',	0.287

(*) – value recalculated from the torsion S-N curve performed on the full round cross-section specimen using the algorithm presented in the next paragraph.

For the constant-amplitude sinusoidal proportional and non-proportional loading, the tests were carried out with a phase shift $\delta = \pi/2$ and frequency $f = 20$ Hz under different ratios of the torsion and bending moments $\lambda_M = M_{t,max}/M_{b,max}$. For the variable-amplitude loading, the specimens were subjected to bending or torsion loading with a normal probability distribution and a narrow frequency band. The fatigue life and the macroscopic fatigue fracture plane orientation was determined for each specimen with the assumption that the fracture plane orientation could be determined from the crack line position observed on the photos of the specimen surface (crack length around 2÷3mm). The experimental results are presented in Tab. 2, where $\hat{\alpha}_{\exp}$ is the averaged value of experimental angles $\alpha_{\exp}$, $< \hat{\alpha}_{\min} \div \hat{\alpha}_{\max} >$ is the confidence interval (assuming a normal distribution of the $\alpha_{\exp}$) which contains 50% of the probability and $\alpha_{\exp}$ is the angle between unit-normal vector $\vec{n}$ to crack plane and the specimen axis **z**.

Two fatigue crack behaviours were noticed: (i) one general crack orientation at the macroscale was observed under all the investigated constant-amplitude loadings and under the variable-amplitude bending; (ii) two crack orientations were observed for the specimens subjected to variable-amplitude torsion. The first orientation with a crack length of around 0.15-0.3 mm is parallel to the specimen axis. The other orientation comes from branching of the primary crack, and these branching directions are inclined to the specimen axis by around 45^o (load case no 7).

Table 2. Experimental data

No	δ rad	$M_{b,max}$ Nm	λ_M -	$\hat{\alpha}_{\exp}$ [°]	$< \hat{\alpha}_{\min} \div \hat{\alpha}_{\max} >$ [°]
Constant-amplitude loading					
1	0	8.0; 10.0; 10.3	0.68	18.1	17.1 ÷ 19.0
2	0	6.4; 7.4; 8.2; 9.8	0.96	21.9	20.0 ÷ 23.8
3	0	5.3; 6.2; 7.2;	1.44	26.5	23.8 ÷ 29.2
4	π/2	8.9; 9.2; 9.6; 10.3	0.68	12.3	9.1 ÷ 15.5
5	π/2	8.3	0.98	8.4	7.3 ÷ 9.5
6	π/2	6.4; 7.2	1.42	10.2	6.4 ÷ 13.9
Variable-amplitude loading					
7	-	18.4	∞	43.6/86.3	42.2÷45.0/82.3 ÷ 90.2
8	-	16.3	0	1.5	0.8÷2.2

STRESS AND STRAIN COMPUTATIONS

Stress and strain histories in an arbitrary point (x, y) of the specimen cross-section were computed from bending and torsion moments $M_b(t)$, $M_t(t)$ considering the plastic strains. Plasticity was included in the computation since the cyclic properties (K', n') of the 18G2A steel reveal the appearance of the plastic strains even under low stress level ($\varepsilon_a^p = 0.65\%$ for $\sigma_{af} = 204$ MPa). The Chu [13] plasticity model of material behaviour was applied to determine the strain-stress relation and the influence of loading history on the strain state for each point of the specimen cross-section. For every increment of bending $\Delta M_b(t)$ and torsion $\Delta M_t(t)$ moments the following quasi-static equilibrium equations were solved by the trust-region method [14]

$$\int_A \Delta\sigma_{zz}(x,y,t)y dA - \Delta M_b(t) = 0\,, \quad \int_A \Delta\tau_{z\phi}(\rho,t)\rho dA - \Delta M_t(t) = 0\,, \tag{21}$$

where the increment Δ is defined as $\Delta\sigma_{zz}(x, y, t) = \sigma_{zz}(x, y, t+\Delta t) - \sigma_{zz}(x, y, t)$ is the normal stress increment for the finite element with the origin in the plane (x, y); $\Delta\tau_{z\varphi}(t, \rho)$ is the shear stress increment for the finite element with the origin determined by the radius $\rho = \sqrt{x^2 + y^2}$; dA is the area of the finite element. More information about the stress and strain computations are presented in [15].

EVALUATION AND DISCUSSION

The variable-amplitude torsion and bending were used to evaluate the damage accumulation hypothesis. Calculated fatigue life T_{cal} according to the failure criterion of the maximum normal stress applied under the variable-amplitude bending is closer to the experimental fatigue life T_{exp} with the application of the Serensen-Kogayev hypothesis than with the Palmgren-Miner one. Moreover, similar results were obtained

by the criterion of the maximum shear stress, i.e. Findley criterion with k=0, applied under the variable-amplitude torsion. Therefore, the Serensen-Kogayev damage accumulation hypothesis is chosen for the estimation of the fatigue life and the critical plane orientation under the multiaxial and uniaxial loadings.

The following error parameters were used to compare the experimental macroscopic fracture plane orientation with the critical plane orientation

$$E_{\alpha}^{(i)} = \left|\hat{\alpha}_{\exp}^{(i)} - \alpha_{cal}^{(i)}\right|, \quad E_{\alpha,m} = \frac{1}{N}\sum_{i=1}^{N} E_{\alpha}^{(i)}, \tag{22}$$

where N is the number of load cases (N = 8). Some criteria exhibit two critical plane orientations in the investigated α range ($\alpha \in$ <-90°, 90°>, $\Delta\alpha$=0.1°). In this case, for the failure fatigue criterion assessment only the critical plane orientation with smaller $E_{\alpha}^{(i)}$ is taken. Absolute difference $E_{\alpha}^{(i)}$ and the mean value $E_{\alpha,m}$ computed according to the analysed criteria are presented in Table 3. Bold face characters are used for error parameters smaller than 5°. Table 3 also includes the maximum normal stress $\sigma_{zz,max}$ and the stress ratio $\lambda_{\tau\sigma} = \tau_{zx,max}/\sigma_{zz,max}$ computed according to the algorithm mentioned in the previous paragraph. An example distribution of the normalized damage degree calculated according to the $\max\{\sigma_n\}$ multiaxial fatigue failure criterion along the α angle is shown in Fig. 1.

Table 3. Error parameters: $E_{\alpha}^{(i)}$, $E_{\alpha,m}$ computed according to the analysed criteria

No	$\sigma_{zz,max}$ MPa	$\lambda_{\tau\sigma}$	Matake, [°] k = 0.4,	Findley, [°], k 0.2	0.4	0.8	1.6	FS, [°]	max{σ_n}, [°]
1	223; 280; 286	0.29	11.8	6.1	**0.9**	7.5	17.2	11.6	**3.0**
2	184; 214; 236; 280	0.44	**2.5**	**3.1**	8.4	16.8	17.3	**2.4**	**1.3**
3	156; 182; 212	0.68	8.3	14.0	19.2	25.3	15.7	8.4	**0.3**
4	262; 272; 281; 295	0,50	22.2	18.0	14.3	7.5	**0.8**	28.4	7.8
5	262	0,62	7.4	58.6	45.4	31.9	20.7	**1.8**	**2.8**
6	250; 278	0,71	10.0	68.9	58.4	42.2	**1.4**	**3.3**	**2.9**
7	0	∞	**0.9**	5.4	10.9	19.3	29.0	**0.0**	**1.4**
8	280	0	43.5	37.8	32.6	24.2	14.6	43.5	**1.5**
		$E_{\alpha,m}$:	13.3	26.5	23.3	21.8	14.6	12.4	**2.6**

The macroscopic fracture plane orientation coincides with the maximum shear stress plane (the Matake criterion) only in the case of the pure torsion. In all other cases, the best correlation between macroscopic fracture plane orientation and the critical plane orientation is obtained by the criterion of the maximum normal stress. The Findley criterion was verified for different values of the k coefficient. With increasing the k value the mean error $E_{\alpha,m}$ decreases. However, the smallest mean error for k = 1.6 is still larger than the result given by the maximum normal stress plane. The influence of the normal stress σ_n on the equivalent Findley stress (Eq. 5) increases with the increasing k value. Therefore, the Findley critical plane orientation approaches to the

experimental fracture plane orientation when the coefficient k increases. The k coefficient cannot increase to infinity since with the increasing k value the damage degree increases.

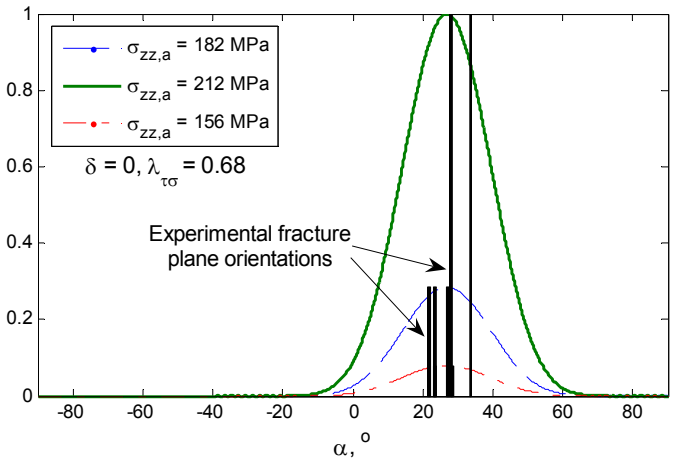

Figure 1. Normalized damage degree calculated according to the $\max\{\sigma_n\}$ multiaxial fatigue failure criterion as a function of the plane orientation.

After the critical plane evaluation, the fatigue failure criteria were used to calculate the fatigue life. The following errors parameters were applied for the fatigue life verification:

$$E^{(i)} = \log\frac{T_{cal}^{(i)}}{T_{\exp}^{(i)}}, \quad E_m = \frac{1}{N}\sum_{i=1}^{N} E^{(i)}, \quad E_{std} = \sqrt{\frac{1}{N-1}\sum_{i=1}^{N}\left(E^{(i)} - E_m\right)^2}. \tag{23}$$

For ideal consistency of the *i-th* calculated fatigue life with the *i-th* experimental fatigue life, the error parameter $E^{(i)}$ is equal to zero. If $E^{(i)}$ is negative, the fatigue life estimation is conservative (safety). The mean error parameter E_m reflects the general results conformity. The standard deviation error parameter E_{std} is the superior parameter since it reflects the scatter of the results and therefore gives us the information about the failure criterion ability to correlate the different kind of multiaxial stress states and the equivalent damage parameter. The second-rate parameter E_m depends on the material constants and the stress gradient.

Fig. 2 (a) presents the comparison between the experimental fatigue lives T_{exp} and the calculated fatigue lives T_{cal} obtained by the maximum normal stress criterion. It is very interesting to notice that the scatter of the results is very small for the specimens that exhibit one macroscopic fracture plane orientation which coincide with the maximum normal stress plane. The results exposed by the criterion of the maximum shear stress (Fig.1 b) show very large scatter $E_{std} = 0.69$ although the mean error is very small $E_m = 0.05$. The other criteria that combine the shear and normal stress/strain components on the critical plane (Findley, Matake, SF) are not appropriate for the steel analysed (Table 4).

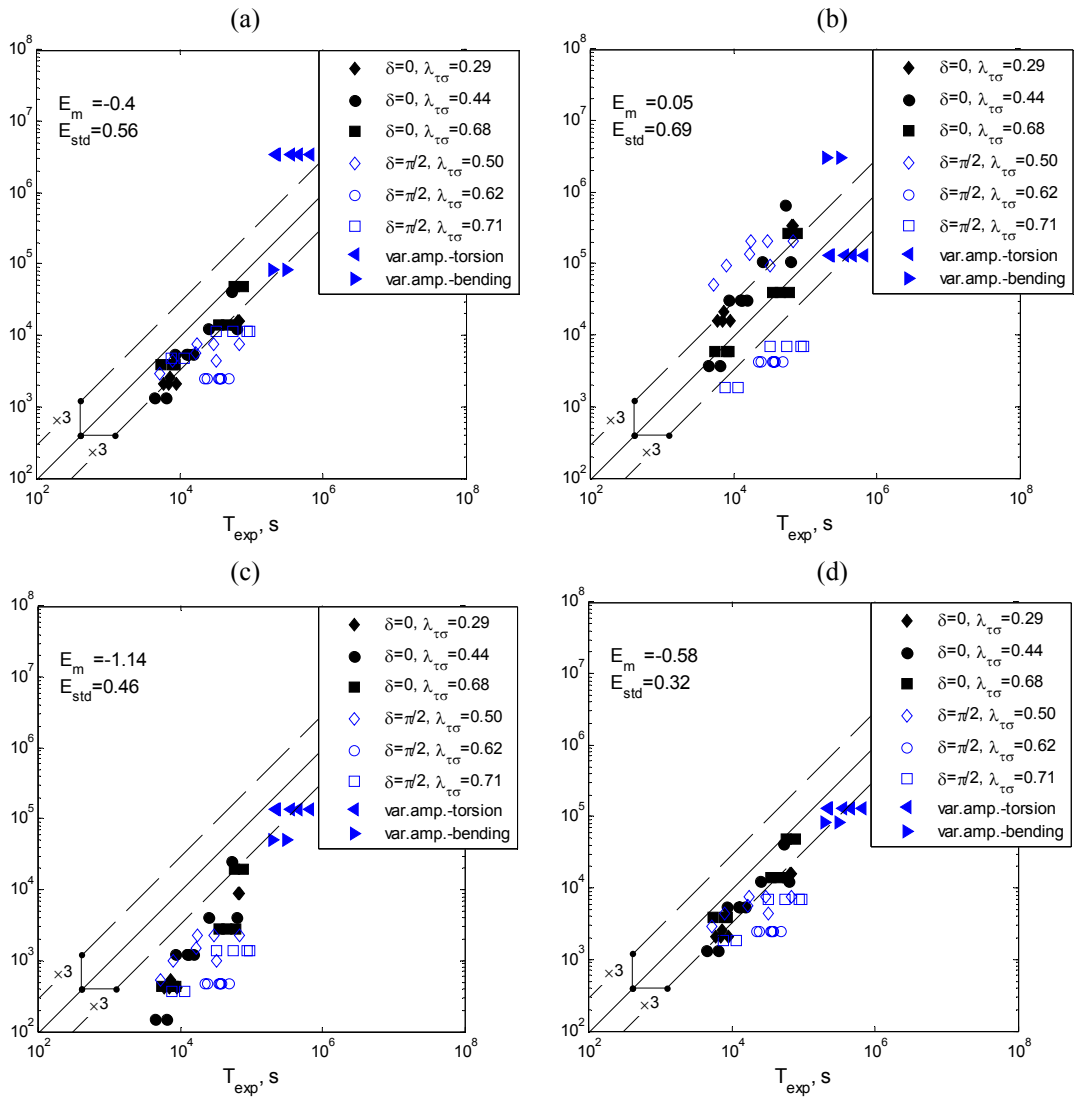

Figure 2. Comparison between the experimental fatigue lives T_{exp} and the calculated fatigue lives T_{cal}: (a) the maximum normal stress criterion, (b) the maximum shear stress criterion (the Findley criterion Eq. 5 for $k = 0$), (c) the Matake criterion Eqs 8 and 10, (d) the max$\{\sigma_n, \tau_{ns}\}$ criterion.

From the engineering point of view, the material fracture behaviour is not known before the material fatigue failure and therefore this feature cannot be used as a key in the selection of the proper fatigue criterion. It was assumed that this selection could be made by the maximum damage degree computed by two simple criteria, i.e. the maximum normal stress criterion (Eq. 13) and the maximum shear stress criterion (Eq. (5) for k=0). For each specimen, the damage degree on the critical plane is computed by these two criteria (max$\{\sigma_n, \tau_{ns}\}$) and than the fatigue life T_{cal} is determined by the highest damage degree (Fig. 2 d).

Table 4. Error life parameters for the analysed multiaxial fatigue failure criteria

	Matake	Findley, k				FS, w			$\max\{\sigma_n\}$	$\max\{\sigma_n, \tau_{ns}\}$
		0.0	0.2	0.4	0.8	0.2	0.4	0.8		
E_{std}	0.46	0.69	0.44	0.43	0.58	1.02	0.97	0.89	0.56	0.32
E_m	-1.14	0.05	-0.60	-1.38	-2.96	-1.58	-1.60	-1.63	-0.40	-0.58

CONCLUSIONS

1. Experimental results expose two material fatigue fracture behaviour: (i) one general crack orientation at the macroscale were observed under all the investigated constant-amplitude loadings ($\lambda_{\tau\sigma}=\tau_{zx,max}/\sigma_{zz,max}\leq 0.71$) and under the variable-amplitude bending; (ii) two crack orientations were observed for the specimens subjected to variable-amplitude torsion.
2. Macroscopic fracture planes under the proportional and non-proportional multiaxial loading for $\lambda_{\tau\sigma}=\tau_{zx,max}/\sigma_{zz,max}\leq 0.71$ reveals the same behaviour as under pure bending.
3. Under investigated test conditions, the experimental and calculated fatigue lives can be successfully correlated by two simple multiaxial fatigue failure criteria based on the critical plane approach, i.e. the criteria of the maximum shear or normal stress.

REFERENCES

1. Karolczuk, A., Macha, E. (2005) Int. J. Fracture **134**, 267-304.
2. Findley, W.N. (1959) *Journal of Engineering for Industry*, November, 301-306.
3. Park, J. and Nelson, D. (2000) *Int. J. Fatigue* **22**, 23-39.
4. Backstrom, M., Marquis, G. (2001) *Fatigue Fract Engng Mater Struct* **24**, 279-291.
5. Banvillet A., Lagoda T., Macha E., NieslonyA., Palin-Luc T., Vittori J.-F. (2004) *Int. J. Fatigue* **26**, 349-363.
6. Carpinteri, A., Spagnoli A. and Vantadori, A.S. (2003) *Fatigue Fract Engng Mater Struct* **26**, 515–522.
7. Matake, T. (1977) *Bulletin of The Japan Society of Mech. Eng.* **20**, 257-263.
8. Fatemi, A. and Socie, D.F. (1988) *Fatigue Fract Engng Mater Struct* **11**, 149–165.
9. Miner, M.A. (1945) *J. Appl. Mech.* **12**, 159-164.
10. Serensen, S.V., Kogayev, V.P. & Shnejderovich, R.M. (1975) *Permissible Loading and Strength Calculations of Machine Components, Third Edn*., Mashinostroenie, Moskva (in Russian).
11. Karolczuk, A., Macha, E. (2005) *Critical Planes in Multiaxial Fatigue of Materials, Monograph*, Fortschritt-Berichte VDI, Mechanik/Bruchmechanik, reihe 18, nr. 298, Dusseldorf: VDI Verlag.
12. Karolczuk, A., Macha, E. (2005) *Fatigue Fract Engng Mater Struct* **28**, 99-106.
13. Chu, CC. (1984) *J. Mech. Phys. Solids*; **32**(3), 197-212.
14. MATLAB. (2004) Optimization Toolbox User Guide, version 6.5, The MathWorks
15. Karolczuk, A. (2006), *Engineering Fracture Mechanics*, (in print).